Capturing patterns of variation unique to a specific dataset

Robin Tu[1], Alexander H. Foss[2], and Sihai Dave Zhao[1]

[1]Department of Statistics, University of Illinois at Urbana-Champaign, Champaign, IL
[2]Statistical Sciences, Sandia National Laboratories, Albuquerque, NM

January 3, 2021

1 Introduction

Capturing patterns of variation present in a dataset is an important step in exploratory data analysis and unsupervised learning. Popular methods include principal component analysis (PCA) [10], nonnegative matrix factorization [13], projection pursuit [9], and independent component analysis [7]. Frequently, however, many of the identified patterns may actually arise from systematic or technical variation, for example batch effects, that are not of substantive interest.

New approaches are necessary for capturing meaningful patterns of variation. A popular approach is to contrast a target dataset of interest with a carefully chosen background dataset that represents unwanted or uninteresting variation. Patterns of variation unique to the target, and not present in the background, are more likely to be substantively meaningful. For example, in Section 2.1, we analyze proteomics data from of normal and trisomic mice that have undergone shock therapy and/or drug therapy. One goal is to identify patterns uniquely associated with normal mice. However, the dominant modes of variation in the dataset arise from the shock treatment and the trisomic gene, which are not of interest. Therefore, we contrast the data with a background dataset of proteomics data from shock-treated and drug-treated trisomic mice. As a result, the remaining patterns of variation unique to the target dataset reveal features specific to normal mice.

This approach was first introduced by Abid et al. [1], who proposed contrastive principal components analysis (cPCA). While standard PCA identifies directions of variation that explain the most variation in the target dataset, cPCA seeks directions that explain more variation in the target than in the background. The most important patterns are those corresponding to the largest gap between the two datasets. Salloum and Kuo [17] later introduced cPCA++, which maximizes the ratio, rather than the difference, of the variance explained by the target and background. Boileau et al. [4] described sparse cPCA, which

seeks maxmially contrastive patterns of variation that can be characterized using a parsimonious set of features. Other types of contrastive implementations include latent models [18] and autoencoders [2].

There are two main issues with existing contrastive methods. First, a major disadvantage is that they cannot accommodate multiple background datasets. Using multiple backgrounds allows researchers to better hone in on the unique variation of interest by removing multiple types or sources of unwanted variation. For example, in the emotion analysis in Section 2.2, where we seek to uncover facial features characterizing the expression of "afraid", the dataset we use also contains background images from six other emotions. If we can simultaneously contrast the target data with multiple other background emotions, we will be able to identify more refined and distinctive patterns of variation characterizing "afraid". Naively applying existing methods by pooling the different emotions into a single background dataset is suboptimal, as variation in the pooled data may not be representative of variation in any of the individual datasets.

The second disadvantage of existing contrastive methods is that they typically require one or more tuning parameters. For example, cPCA requires the user to specify how much to penalize patterns that explain a large amount of variation in the background data. It is not clear in general how to choose these tuning parameters objectively.

We propose Unique Component Analysis (UCA), which addresses both of these issues. Not only can UCA contrast a target dataset against multiple backgrounds, but it also does not require any tuning parameters. UCA finds directions of variation that maximize the explained variation in the target under a constraint on the amount of variation they can explain in each of the backgrounds. With a single background, UCA is equivalent to cPCA but with an automatically selected tuning parameter. We show that UCA achieves similar results as cPCA and cPCA++ with a single background and that it can outperform them when using multiple backgrounds. We also develop computationally scalable algorithms for application to experiments with large numbers of measured features.

2 Results

2.1 Discovering subgroups in protein expression data

We applied UCA to mouse proteomics data, which were also used by Abid et al. [1] to illustrate cPCA performance. The study measured levels of 76 proteins in 1080 normal and trisomic (Down Syndrome) mice receiving various combinations of therapy (shock vs. no shock) and drug (memantine vs. saline) [3, 12, 1]. The goal of the experiment was to assess whether memantine improved learning ability in trisomic mice and to identify subsets of protein that may be involved in this process.

Just confirming that the text description of the analysis no longer flips shock and unshock?

We first replicate the analysis by Abid et al. [1]. We want to extract patterns of variation in protein levels that can help discriminate normal from trisomic mice. Our target dataset consisted of protein data from unshocked mice given saline. However, natural variation, arising from factors such as age and gender, may dominant this dataset and obscure the
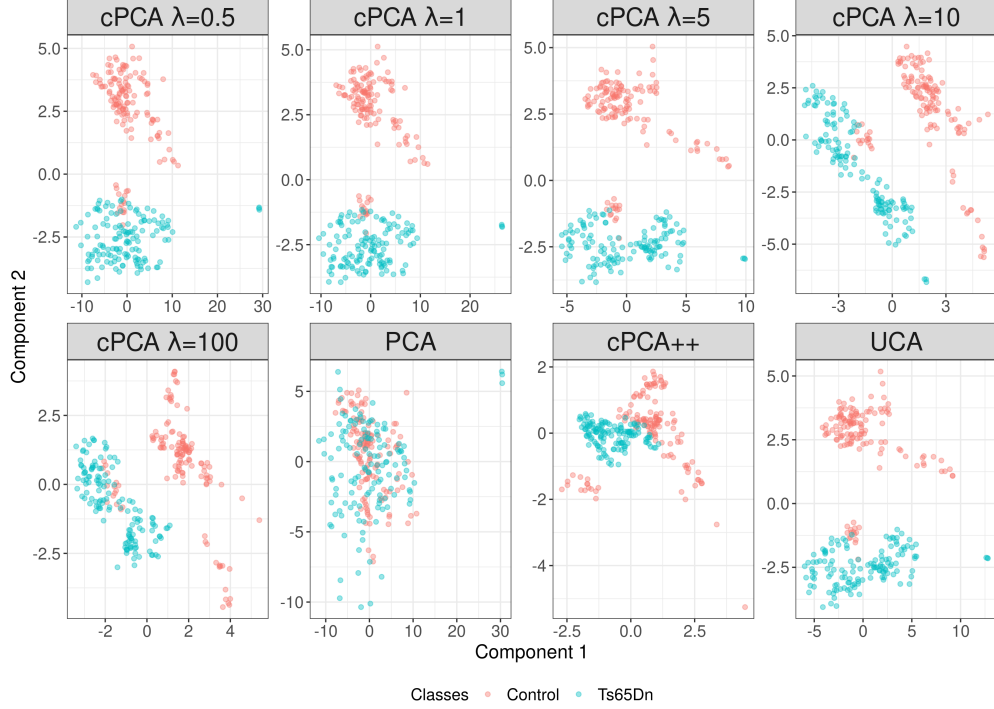
Figure 1: Mouse Protein Expression: Down Syndrome (Ts65Dn) separability of saline in-jected mice which were not subject to shock therapy. Down Syndrome and control mice were unseparable using PCA alone but is easily separable by cPCA at all values of the contrastive parameter λ. The mice are also easily separable by cPCA++ and UCA.

variation of interest due to trisomy. To remove this natural variation, we contrasted the target data with a background dataset consisting of normal mice who had been given saline but had also been shocked. As natural variation is likely present in both the target and the background, patterns that explaining variation in the target but not the background may be more likely to related to trisomy.

Figure 1 shows the data projected to the first two components identified by PCA, cPCA, cPCA++, and UCA. Normal and trisomic mice are not well-separated in the PCA results, showing that dominant variation in the target data indeed does not stem from trisomy. In contrast, the two mouse groups are much more clearly separated in the cPCA results. While this separation is noticeable for each of the tuning parameter values we tried, the actual projected data can vary considerably, and the optimal tuning parameter value remains unclear. cPCA++, which does not require specifying tuning parameter here because the number of samples exceeds the number of features, shows better separation than PCA but does not perform as well as cPCA. UCA performs as well as cPCA but without requiring a tuning parameter.

We next repeat the same analysis, but this time using shocked mice given saline as our target dataset. Abid et al. [1] did not consider this analysis, where separating normal and trisomic shocked mice proves to be a much more challenging problem. Figure 2 shows that normal and trisomic mice are again not well-separated by the first two components learned by PCA. Here we extract patterns of variation unique to normal mice and so applied UCA
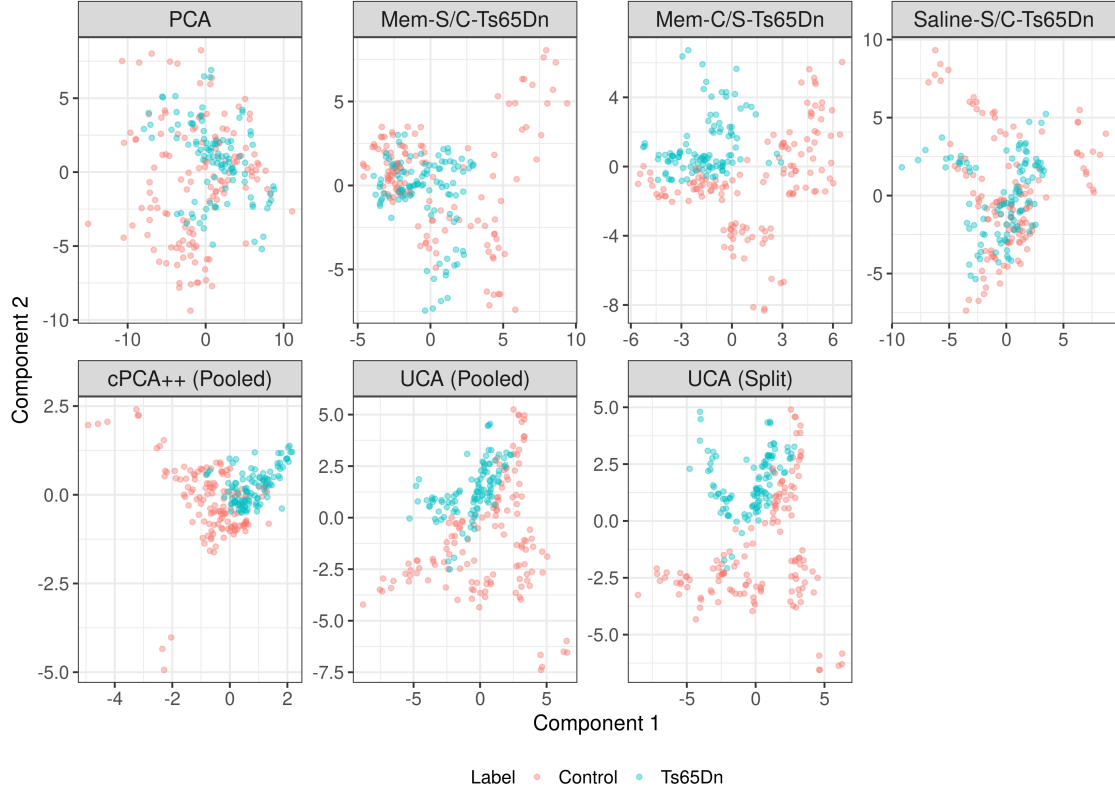
3

Figure 2: Mouse Protein Expression: Separability of normal and trisomic mice that were shocked injected with saline. Background datasets: unshocked trisomic mice injected with memantine (Mem-S/C-Ts65Dn), shocked trisomic mice injected with memantine (Mem-C/S-Ts65Dn), and unshocked trisomic mice injected with saline (Saline-S/C-Ts65Dn). Pooled: all background datasets are pooled into one background. Split: UCA using multiple separate individual backgrounds.

using three trisomic mouse datasets as backgrounds.

The results show that a single background dataset alone cannot separate normal and trisomic mice well. Pooling the three individual backgrounds together achieves slightly better separability compared to some of the individual backgrounds. However, natively constrasting multiple backgrounds simultaneously without pooling allows our proposed UCA to remove variability specific to each background and results in the best separability.

2.2 Discovering eigenfaces of emotion

We further illustrate the advantages of contrasting multiple background datasets with UCA using the Karolinska Directed Emotional Faces (KDEF) [6], which captured images of seven emotions from five different angles from 70 amateur actors in either a practice or final session. Figure 3b presents averaged images of each emotion calculated from all female actors in their final session.

We focus on uncovering variation unique to the "afraid" emotion using all final session

pictures from every emotion from female actors. Since this target contains six other emotions, standard PCA will not provide variation unique to "afraid". Instead, we leverage images from the practice session to serve as background data. We construct six separate backgrounds, corresponding to the six other emotions, and contrast out their variation using UCA. For comparison, we also pooled these images together into a single background dataset and performed UCA using the pooled background.
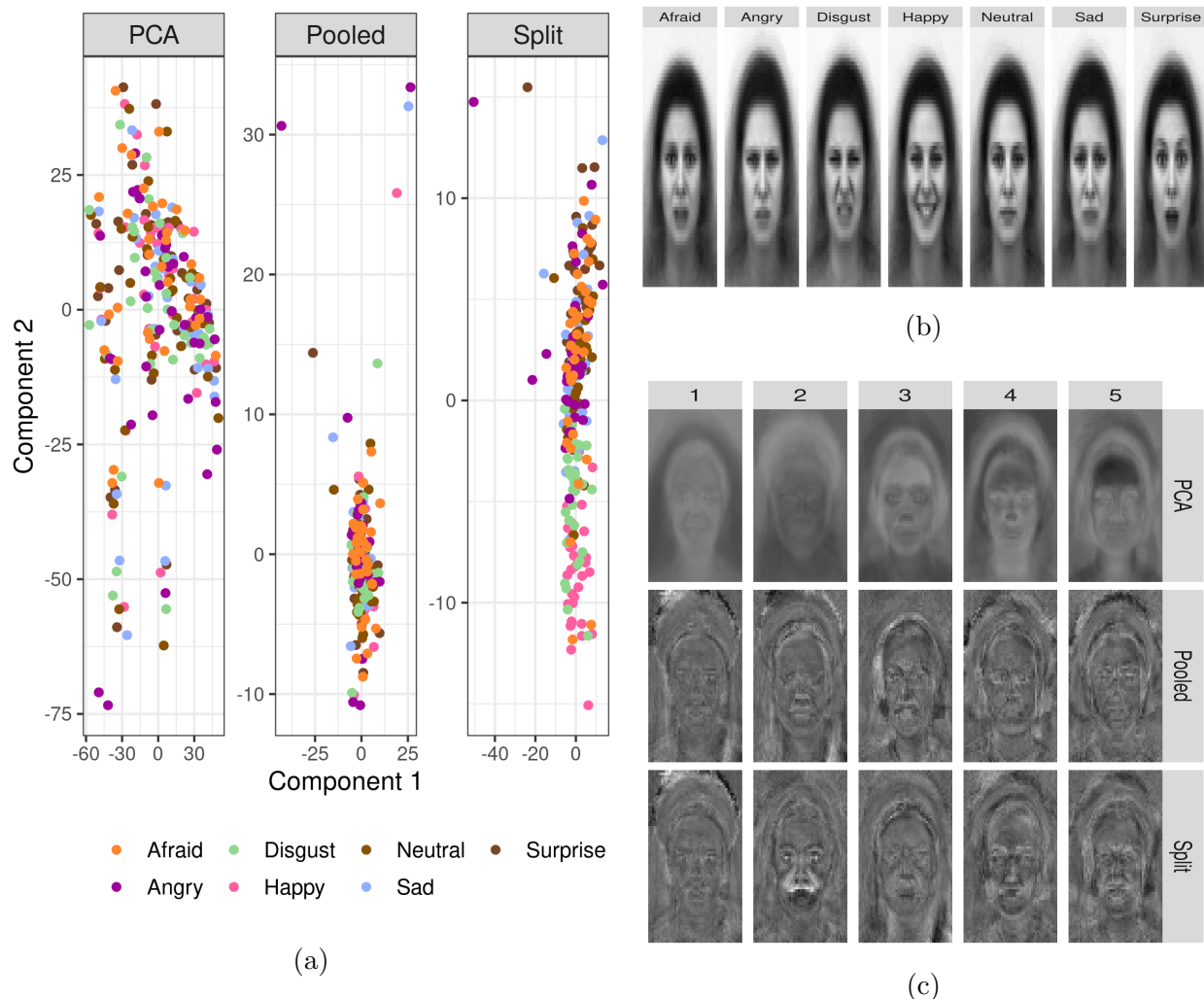

Figure 3: **The faces in (b) look too squashed. Can you come up with a different arrangement of the subfigures? Also since some of the colors in the PCA are too similar, I had another idea, do you think we can do shapes as well? So like the "bad" emotions (anger, digust, etc.) get different shapes?** Results of analysis of KDEF faces. (a) Faces projected onto the first two components found by PCA, UCA with a pooled background, and UCA using multiple backgrounds. (b) Each emotion averaged over all female actors. (c) Top 5 eigenfaces of female emotions produced by different analyses.

Figure 3a projects the target data onto the first two directions of variation calculated using each method. The emotions are entirely intermixed when projected onto components produced by PCA and by UCA using a single pooled background. In contrast, the emotions

are much more separable when using UCA with multiple separate backgrounds. In particular, "afraid" faces are very separate from the "disgust" and "happy" faces. This indicates that UCA with multiple backgrounds can identify patterns of variation that can distinguish "afraid" from the other emotions.

Figure 3c shows visualizes the top five directions of variation produced by each method as faces. These are called eigenfaces, and this visualization technique is useful for interpreting the top components as facial features [19]. PCA eigenfaces generally represent features common to all the emotions. UCA eigenfaces using a pooled background seem to highlight the eyebrows and upper lips, though it is difficult to discern. On the other hand, eigenfaces produced using UCA using multiple separate backgrounds highlight eyebrows, eyes, nostrils, and nasolabial folds. These are especially clear in the second eigenface and accord with intuition about which features would likely be most useful in distinguishing "afraid" from other emotions.

3 Discussion

In many data analytics settings, we are interested in removing uninteresting variation that contaminate the data of interest. Here we proposed UCA, a tuning-free contrastive learning method that can accommodate multiple background datasets. We showed in analyses of mouse proteomics data and facial image data that UCA performs as well as cPCA when used with a single background dataset but can have dramatically better performance when used with multiple separate backgrounds.

We have released the code for UCA as an R package, along with documentation and examples. Like cPCA, the choice of background still plays a pivotal role in the directions found by UCA.

Conclusion seems too short, do you have anything else to add? What does the original cPCA paper have in their discussion?

4 Method

4.1 Contrastive principal components analysis

We first briefly review cPCA [1]. Let A denoted the $p \times p$ sample covariance matrix constucted from target data $X_{n_x \times p}$ and B denote the $p \times p$ sample background covariance constructed from background data $Y_{n_y \times p}$. The goal of cPCA is to find the directions of variability, $v \in \mathbb{R}^p$, which account for large variation in the target data Y and small variation in the background data X where $\|v\|_2 = 1$. Specifically, for some parameter λ, cPCA seeks the eigenvectors v solving

$$\arg\max_{v \in \mathbb{R}^p} \left(v^T A v - \lambda v^T B v \right) = \arg\max_{v \in \mathbb{R}^p} v^T \left(A - \lambda B \right) v.$$

For a given λ, the direction is simply the eigenvector of the weighted difference between covariance matrices where v maximize the variation in A while constraining variation in B.

The tuning parameter λ measures how much to penalize the background data covariance. When $\lambda = 0$, background variation isn't accounted for, thus the cPCA is reduced to PCA. As

λ increases, the relative background variation becomes more dominant, causing v_λ **What's v_λ? Need to define it** to focus on directions which minimize background variation rather than maximizing the target. For very large values of λ, v_λ is equivalent to PCA after projecting the target data onto the nullspace of the background data. The authors of cPCA suggested that λ be chosen using spectral clustering via a parameter sweep of logarithmically spaced candidate values.

4.2 Unique Component Analysis

We introduce the Unique Component Analysis (UCA) framework to identify the optimal contrastive parameter, λ, and the resulting directions of variation using the duality of lagrangians. By adding the additional constraints of $v^T v = 1$ and $v^T B v = 1$ we arrive at an objective method to choose λ. These constraints are motivated by similar constraints in generalized eigenvalue problems, e.g. PCA where $Av = \lambda I v$ enforces $v^T v = 1$, cPCA++ where $Av = \lambda B v$ which enforces $v^T B v = 1$. **Why does cPCA++ enforce $v^\top B v = 1$? We should explain.** Constraining $v^T v = 1$ while $v^T B v$ is unconstrained may result in eigenvectors that explain large amounts of variability in the target but also explain large amounts of variability in the background. However, constraining $v^T B v = 1$ while leaving $v^T v$ unconstrained results in eigenvectors that are not norm 1 and explain near zero variability in the target. **How is this possible? Need to explain. Basically we need to explain how cPCA++ works before we explain UCA.**

UCA combines both of these constraints together and can be expressed as a primal optimization problem:

$$\max_{v \in \mathbb{R}^p} v^T A v \tag{1}$$
$$\text{subject to } v^T v = 1, \quad v^T B v \leq 1$$

We can solve 1 using weak duality of Lagrangians, $\mathcal{L}$:

$$\max_{\lambda \geq 0} \max_{v \in \mathbb{R}^P} \mathcal{L}(v, \lambda) = \max_{\lambda \geq 0} \max_{v \in \mathbb{R}^P} \left(v^T A v - \lambda \left(v^T B v - 1 \right) \right)$$
$$= \max_{\lambda \geq 0} \max_{v \in \mathbb{R}^P} \left(v^T (A - \lambda B) v + \lambda \right)$$
$$= \max_{\lambda \geq 0} \left(\lambda_{\max}(A - \lambda B) + \lambda \right) \tag{2}$$

where λ is the Lagrange multiplier associated with the constraint $v^T B v \leq 1$ and $\lambda_{max}(A - \lambda B)$ is the largest eigenvalue associated with $A - \lambda B$. Although we have two constraints, we get $v^T v = I$ through eigendecomposition. **This section contains some errors. You're proposing to solve the primal problem by appealing to weak duality. But I think weak duality is not enough to guarantee that solving the dual problem can help you solve the primal problem. You need strong duality. Does strong duality hold?**

Also, it's not immediately clear where you used a eigendecomposition. An eigendecomposition is a factorization of a matrix $M = V \Sigma V^\top$, but I don't see a matrix factorization here. I think you can be more precise about what exactly you did.

To solve (2), we can take the derivative of the Lagrangian $\mathcal{L}$ with respect to λ **This is not true, you are not taking a derivative of $\mathcal{L}(u, v)$, you're taking a derivative of $\max_v \mathcal{L}(u, v)$, which is way different and much harder** and set the derivative equal to zero:

$$
\begin{aligned}
\frac{\partial}{\partial \lambda} \max_{v \in \mathbb{R}^P} \mathcal{L}(v, \lambda) &= \frac{\partial}{\partial \lambda} \left(\lambda_{max} (A - \lambda B) + \lambda \right) \\
&= \frac{\partial}{\partial \lambda} \left(v_\lambda^T (A - \lambda B) v_\lambda + \lambda \right) \\
&\Leftrightarrow \frac{\partial}{\partial \lambda} \left(-\lambda v_\lambda^T B v_\lambda + \lambda \right) \\
&= 1 - v_\lambda^T B v_\lambda = 0
\end{aligned}
\tag{3}
$$

where v_λ is the eigenvector associated with the largest eigenvalue for particular λ.

We use an iterative algorithm (L-BFGS-B) [5] to optimize between finding the Lagrange Multiplier λ, and finding the associated eigenvectors v_λ, stopping when equation 3 is satisfied. **How do you know that this interation between λ and v_λ will converge, and if it converges, how do you know it will converge to a global rather than local optimum?** With the optimal Lagrange Multiplier, eigenvector v_λ maximizes equation 1. Thus our constraints allows for a natural way to pick the contrastive parameter λ in cPCA.

Similarly, for multiple backgrounds, again let the A be the target $p \times p$ covariance matrix and $B_1, \ldots, B_m$ be the m background $p \times p$ covariance matrices constructed from a $n_y \times p$ dimensional Y data matrix and corresponding $(n_{x_1} \times p), \ldots, (n_{x_m} \times p)$ dimensional $X_1, \ldots, X_m$ background data matrices.

We add additional constraints $v^T B_j v \leq 1$ to our optimization problem 1 for each background $j = 1, \ldots, m$. Specifically, the primal problem becomes

$$
\max_{v \in \mathbb{R}^p} v^T A v
\tag{4}
$$
$$
\text{subject to} \quad v^T v = 1, \quad v^T B_1 v \leq 1, \ldots, v^T B_m v \leq 1
$$

The corresponding dual problem is

$$
\begin{aligned}
\max_{\lambda_1, \ldots, \lambda_m \geq 0} \max_{v \in \mathbb{R}^P} \mathcal{L}(v, \lambda_1, \ldots, \lambda_m) &= \max_{\lambda_1, \ldots, \lambda_m \geq 0} \max_{v \in \mathbb{R}^P} \left(v^T \left(A - \sum_{j=1}^m \lambda_j B_j \right) v + \sum_{j=1}^m \lambda_j \right) \\
&= \max_{\lambda_1, \ldots, \lambda_m \geq 0} \left(\lambda_{\max} \left(A - \sum_{j=1}^m \lambda_j B_j \right) + \sum_{j=1}^m \lambda_j \right)
\end{aligned}
\tag{5}
$$

For background $j \in 1, \ldots, m$, we can solve for the jth Lagrange multiplier in equation 5

similarly by taking the partial derivative and setting to zero:

$$\frac{\partial}{\partial \lambda_j}\left(\lambda_{\max}\left(A - \sum_{j=1}^{m}\lambda_j B_j\right) + \sum_{j=1}^{m}\lambda_j\right) = \frac{\partial}{\partial \lambda_j}v_\lambda^T\left(A - \sum_{j=1}^{m}\lambda_j B_j\right)v_\lambda + \sum_{j=1}^{m}\lambda_j$$

$$\Leftrightarrow \frac{\partial}{\partial \lambda_j}\left(v_\lambda^T\left(A - \lambda_j B_j\right)v_\lambda + \lambda_j\right)$$

$$\Leftrightarrow \frac{\partial}{\partial \lambda_j}\left(-\lambda_j v_\lambda^T B_j v_\lambda + \lambda_j\right)$$

$$= 1 - v_{\lambda_j}^T B_j v_{\lambda_j} = 0 \tag{6}$$

To solve this multiple background dataset problem we propose a coordinate descent algorithm that utilizes the single background dataset L-BFGS-B [5] algorithm iteratively. **Again, how do you know that this coordinate descent algorithm will converge to a global optimum?** For m background datasets, on the qth iteration, let $A_{(j)}^*$ be the variation in A after excluding background variation that is not B_j:

$$A_{(j)}^* = A - \sum_{i=1}^{j-1}\lambda_i^{(q+1)}B_i - \sum_{i=j+1}^{m}\lambda_i^{(q)}B_i$$

to solve for j^{th} of the m Lagrange multipliers, we use Algorithm 1.

4.3 Extension to High Dimensional Data:

First need to explain what the problem is when we have high-dimensional data. Actually first need to explain what high-dimensional data means. To extend our method to high-dimensional data, we avoid the traditional eigendecomposition method of finding eigenvalue/eigenvectors of the covariance matrix. Just like how singular-value decomposition (SVD) of the data matrix can be used to find the top eigenvalue/eigenvectors of its covariance, we introduce the Product SVD method to exploit the structure of how the contrastive covariance matrices are formed and employ SVD of a product of matrices to quickly find our top eigenvalue. Breaking the problem down in this way considerably speeds up our L-BFGS-B algorithm, and allows us to run UCA even in the high-dimensional setting.

For a single background, let the $p \times p$ covariance matrices A be the target covariance matrix and B be the background covariance matrix. A and B are formed from corresponding centered $n_y \times p$ target data matrix Y, and centered $n_x \times p$ background data matrix X. We can write the difference of the covariance matrices $A - \lambda B$ as a product of a $p \times (n_y + n_x)$ dimensional left matrix , L, and a $(n_y + n_x) \times p$ dimensional right matrix, R as seen in equation 7:

$$C_\lambda = A - \lambda B$$

$$= \frac{1}{n_y}Y^T Y - \frac{\lambda}{n_x}X^T X$$

$$= \underbrace{\left[\frac{1}{\sqrt{n_y}}Y^T, -\frac{\lambda}{\sqrt{n_x}}X^T\right]}_{L}\underbrace{\begin{bmatrix}\frac{1}{\sqrt{n_y}}Y \\ \frac{1}{\sqrt{n_x}}X\end{bmatrix}}_{R} \tag{7}$$

9

Algorithm 1: coordinate descent algorithm

 Inputs: m centered background data $X_1, \ldots, X_m$, centered Target data Y, k number of components;

Initialize $\lambda_1^{(0)}, \ldots, \lambda_m^{(0)}$, ϵ;

Compute the emperical covariance matrices:

$$A = \frac{1}{n_y} Y^T Y, \;\; B_1 = \frac{1}{n_{x_1}} X_1^T X_1, \;\ldots, B_m = \frac{1}{n_{x_m}} X_m^T X_m$$

while $l^{(q+1)} - l^{(q)} > \epsilon$ **do**

   for $j = 1 : m$ **do**

      Solve for $\lambda_j^{(q+1)}$ via L-BFGS-B, corresponding to the largest eigenvalue of

$$C_{\lambda_j} = A_{(j)}^* - \lambda_j^{(q+1)} B_j$$

   After iterating through m Lagrange Multipliers, calculate value of Lagrangian

$$l^{(q+1)} = \lambda_{max} \left(A - \sum_{j=1}^{m} \lambda_j^{(q+1)} B_j \right) + \sum_{j=1}^{m} \lambda_j^{(q+1)}$$

Compute

$$C_{\lambda_1, \ldots, \lambda_m} = A - \sum_{j=1}^{m} \lambda_j B_j$$

   Find $V_k \in \mathbb{R}^k$, spanned by the top k eigenvectors of $C_{\lambda_1, \ldots, \lambda_k}$;

 Return: V_k

With this formulation, we can follow the steps in Golub et al. [11], and find the singular values and vectors of C_λ using a sequence of SVD and QR decompositions operating on the left and right matrices. Since singular values and eigenvalues coincide in square matrices, we use the singular vectors, U, to find the largest eigenvalues by sorting the diagonal of $ULRU^T$. We describe the Product SVD Method in algorithm 2, which can directly replace the more computationally expensive eigendecomposition in high dimensions.

Similarly, for multiple backgrounds, again let the A be the target $p \times p$ covariance matrix and $B_1, \ldots, B_m$ be the m background $p \times p$ covariance matrices constructed from a $n_y \times p$ dimensional Y data matrix and corresponding $(n_{x_1} \times p), \ldots, (n_{x_m} \times p)$ dimensional $X_1, \ldots X_m$ background data matrices.

We can construct $C_{\lambda_1, \ldots, \lambda_m} = A - \sum_{j=1}^{m} \lambda_j B_j$ analogously by appending the additional
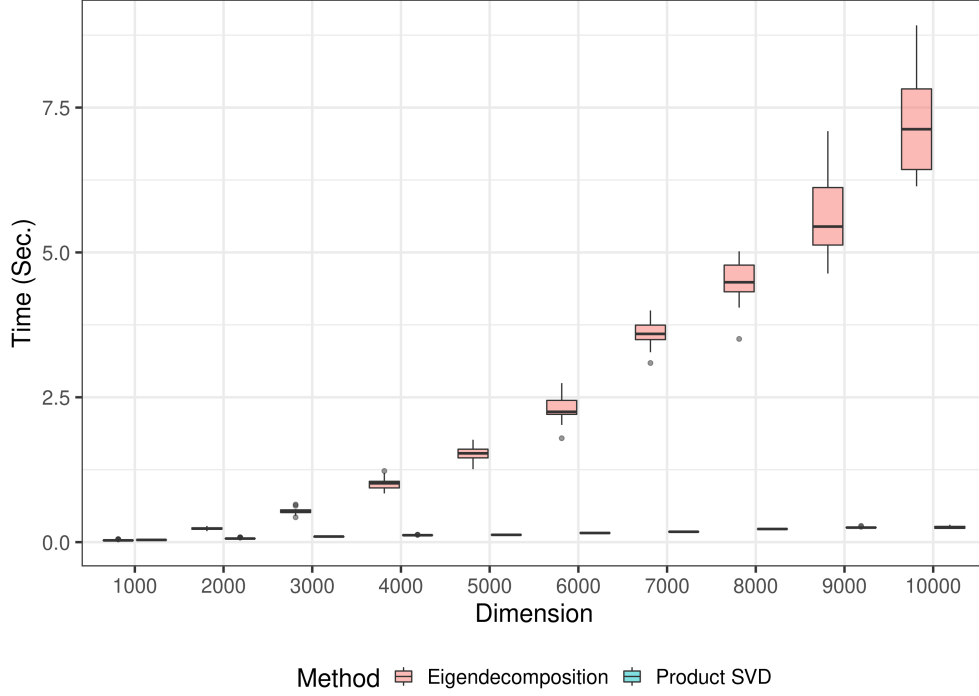
Figure 4: UCA and cPCA implementation using Product SVD vs. eigendecomposition for high-dimensional data: 25 random $100 \times p$ target and background matrices are generated from a standard normal distribution and where p, the dimension varied from 1,000 to 10,000 in steps of 1,000. Box plots of time (in seconds) is plotted for both eigendecomposition and the product SVD method. For small p, there is a negligible difference between the methods. However, as dimension p increases, the Product SVD is significantly faster.

datasets to the left and right matrices:

$$
\begin{aligned}
C_{\lambda_1,\ldots,\lambda_m} &= A - \sum_{j=1}^{m} \lambda_j B_j \\
&= \frac{1}{n_y} Y^T Y - \sum_{j=1}^{m} \frac{\lambda_j}{n_{x_j}} X_j^T X_j \\
&= \underbrace{\left[\frac{1}{\sqrt{n_y}} Y^T, -\frac{\lambda_1}{\sqrt{n_{x_1}}} X_1^T, \ldots, -\frac{\lambda_m}{\sqrt{n_{x_m}}} X_m^T \right]}_{L} \underbrace{\begin{bmatrix} \frac{1}{\sqrt{n_y}} Y \\ \frac{1}{\sqrt{n_{x_1}}} X_1 \\ \vdots \\ \frac{1}{\sqrt{n_{x_m}}} X_m \end{bmatrix}}_{R}
\end{aligned}
\tag{8}
$$

Using the coordinate descent (algorithm 1) to solve for each λ_j prescribed above, we can substitute the eigendecomposition of the covariance matrix, C_{λ_j} with the Product SVD method (algorithm 2) using L and R defined in equation 8.

The Product SVD method is advantageous in high-dimensions because it never explic-

11

Algorithm 2: Product SVD Method to calculate the largest Eigenvalue of C_λ

Input: Centered background matrix X, centered target matrix Y, and λ;

1 Construct $L = \left[\frac{1}{\sqrt{n_y}}Y^T, -\frac{\lambda}{\sqrt{n_x}}X^T\right]$, $R = \begin{bmatrix} \frac{1}{\sqrt{n_y}}Y \\ \frac{1}{\sqrt{n_x}}X \end{bmatrix}$;

2 SVD the right matrix, $R = U_R S_R V_R^T$;

3 QR decompose LU_R into $Q_{LU_R} R_{LU_R}$;

4 SVD the product of R_{LU_R} (step 3) and S_R (step 2), $R_{LU_R}S_R = EDF^T$;

5 The singular vectors of C_λ is the product of Q (step 3) and E (step 4), $U_{C_\lambda} = Q_{LU_R}E$;

6 Find the largest eigenvalues of C_λ by sorting the diagonal of D_{C_λ}, where $D_{C_\lambda} = U_{C_\lambda} C_\lambda U_{C_\lambda}^T$;

Output: $\lambda_{\max}(C_\lambda)$

---

itly operates on the entire $p \times p$ covariance matrix. Not only is our method more memory efficient, scaling with $n \times p$ bytes rather than p^2 bytes, but our method is also computationally more efficient at finding the largest eigenvalue/eigenvector as operating SVD and QR decomposition on either the left or right matrices is faster than directly operating eigendecomposition on the covariance matrix. In the single background scenario, λ only appears in L. Thus since, R doesn't change, we can pre-compute the SVD of R, and only update L when solving for $\lambda_{\max}$. Similarly, in the multi-background scenario, rather than modifying A^* in the original coordinate descent algorithm, this method allows us to only modify the $j + 1$ element of the left data matrix, L. The SVD of the right matrix, R, only needs to be computed once in our coordinate descent. Furthermore, at each step within the coordinate descent only step 3 and 4, the SVD and QR, are computed, and are done on matrices with dimensions much smaller than $p \times p$.

To demonstrate the speed improvements of the Product SVD method compared to the current fastest implementations of eigendecomposition in high-dimensions, we conduct a simulation study with 25 sample $100 \times p$ target and background data matrices generated from a standard Normal distribution with p varying from 1.000 to 10,000 in steps of 1,000. To ensure a fair comparison, we leverage C++ in both implementations using a custom RcppArmadillo [8] function for the Product SVD method and the RSpectra package (0.16-0) [15] for the eigendecomposition method; RSpectra being a package designed for large-scale eigendecompositions based off the C++ Spectra library. We use the microbenchmark package [14] to ensure accurate timings. Our benchmark does not take into account the additional cost of forming the $p \times p$ covariance matrices, which would only exacerbate the difference between the two methods in real world applications.

Figure 4 show box plots of time (in seconds) versus the dimension, p, colored by method, summarizes the results of the simulation study. As dimension p increases, the computational time of our Product SVD method increases much slower than the current eigendecomposition implementations. It should be mentioned that for $p < 1000$ the Product SVD method is slower due to overhead of additional computation on small matrices. In general, for low-dimensional settings where $n \geq p$, the Product SVD will be negligibly slower because of the additional QR, SVD, matrix products, and sort computations.

All computations in this paper were done with R 3.6.3 [16] on an AMD Ryzen 1700X 3.7 gHz processor and 64GB 3000 mhz DDR4 RAM, utilizing the Intel MKL libraries.

I think you should explicitly write out the URLs in addition to links, that's what I usually see people doing.

4.4   Code Availability

We have released a R implementation of . We have implemented both Product SVD on the data matrix and eigendecomposition on the contrastive covariance matrix and allow the background to take either a single background or a list of backgrounds. The GitHub repository also includes R markdown and datasets that reproduce most of the figures in this paper and in the Supplementary.

4.5   Data availability

Datasets that have been used to evaluate UCA in this paper are publicly available from the authors of the original studies. The mouse proteomics data are available from the [**?**]Higuera and the Karolinska Directed Emotional Faces (KDEF) are available from the website [6].

References

[1] Abubakar Abid, Martin J. Zhang, Vivek K. Bagaria, and James Zou. Exploring patterns enriched in a dataset with contrastive principal component analysis. *Nature Communications*, 9:2134, 05 2018.

[2] Abubakar Abid and James Zou. Contrastive variational autoencoder enhances salient features, 2019.

[3] Md. Mahiuddin Ahmed, A. Ranjitha Dhanasekaran, Aaron Block, Suhong Tong, Alberto C. S. Costa, Melissa Stasko, and Katheleen J. Gardiner. Protein dynamics associated with failed and rescued learning in the ts65dn mouse model of down syndrome. *PLOS ONE*, 10(3):1–25, 03 2015.

[4] Philippe Boileau, Nima S Hejazi, and Sandrine Dudoit. Exploring high-dimensional biological data with sparse contrastive principal component analysis. *Bioinformatics*, 36(11):3422–3430, 03 2020.

[5] Richard H Byrd, Peihuang Lu, Jorge Nocedal, and Ciyou Zhu. A limited memory algorithm for bound constrained optimization. *SIAM Journal on scientific computing*, 16(5):1190–1208, 1995.

[6] Manuel G. Calvo and Daniel Lundqvist. Facial expressions of emotion (kdef): Identification under different display-duration conditions. *Behavior Research Methods*, 40(1):109–115, Feb 2008.

[7] Pierre Comon. Independent component analysis, a new concept? *Signal Processing*, 36(3):287 – 314, 1994. Higher Order Statistics.

[8] Dirk Eddelbuettel and Conrad Sanderson. Rcpparmadillo: Accelerating r with high-performance c++ linear algebra. *Computational Statistics and Data Analysis*, 71:1054–1063, March 2014.

[9] J. H. Friedman and J. W. Tukey. A projection pursuit algorithm for exploratory data analysis. *IEEE Transactions on Computers*, C-23(9):881–890, 1974.

[10] Karl Pearson F.R.S. Liii. on lines and planes of closest fit to systems of points in space. *The London, Edinburgh, and Dublin Philosophical Magazine and Journal of Science*, 2(11):559–572, 1901.

[11] Gene Golub, Knut Solna, and Paul Van Dooren. Computing the svd of a general matrix product/quotient. *SIAM Journal on Matrix Analysis and Applications*, 22(1):1–19, 2000.

[12] Clara Higuera, Katheleen J. Gardiner, and Krzysztof J. Cios. Self-organizing feature maps identify proteins critical to learning in a mouse model of down syndrome. *PLOS ONE*, 10(6):1–28, 06 2015.

[13] Daniel D. Lee and H. Sebastian Seung. Learning the parts of objects by non-negative matrix factorization. *Nature*, 401(6755):788–791, Oct 1999.

[14] Olaf Mersmann. *microbenchmark: Accurate Timing Functions*, 2019. R package version 1.4-7.

[15] Yixuan Qiu and Jiali Mei. *RSpectra: Solvers for Large-Scale Eigenvalue and SVD Problems*, 2019. R package version 0.16-0.

[16] R Core Team. *R: A Language and Environment for Statistical Computing*. R Foundation for Statistical Computing, Vienna, Austria, 2020.

[17] Ronald Salloum and C.-C. Jay Kuo. Efficient image splicing localization via contrastive feature extraction. *CoRR*, abs/1901.07172, 2019.

[18] Kristen A Severson, Soumya Ghosh, and Kenney Ng. Unsupervised learning with contrastive latent variable models. In *Proceedings of the AAAI Conference on Artificial Intelligence*, volume 33, pages 4862–4869, 2019.

[19] Matthew Turk and Alex Pentland. Eigenfaces for recognition. *Journal of cognitive neuroscience*, 3(1):71–86, 1991.